AIP | Review of Scientific Instruments

Damage threshold of coating materials on x-ray mirror for x-ray free electron laser

Takahisa Koyama, Hirokatsu Yumoto, Takanori Miura, Kensuke Tono, Tadashi Togashi, Yuichi Inubushi, Tetsuo Katayama, Jangwoo Kim, Satoshi Matsuyama, Makina Yabashi, Kazuto Yamauchi, and Haruhiko Ohashi

Citation: Review of Scientific Instruments **87**, 051801 (2016); doi: 10.1063/1.4950723
View online: http://dx.doi.org/10.1063/1.4950723
View Table of Contents: http://scitation.aip.org/content/aip/journal/rsi/87/5?ver=pdfcov
Published by the AIP Publishing

Damage threshold of coating materials on x-ray mirror for x-ray free electron laser

Takahisa Koyama,[1,2,a)] Hirokatsu Yumoto,[1,2] Takanori Miura,[1] Kensuke Tono,[1,2] Tadashi Togashi,[1,2] Yuichi Inubushi,[1,2] Tetsuo Katayama,[1,2] Jangwoo Kim,[3] Satoshi Matsuyama,[3] Makina Yabashi,[1,2] Kazuto Yamauchi,[3] and Haruhiko Ohashi[1,2]
[1]*Japan Synchrotron Radiation Research Institute (JASRI), 1-1-1 Kouto, Sayo-Cho, Sayo-Gun, Hyogo 679-5198, Japan*
[2]*RIKEN SPring-8 Center, 1-1-1 Kouto, Sayo-Cho, Sayo-Gun, Hyogo 679-5148, Japan*
[3]*Department of Precision Science and Technology, Graduate School of Engineering, Osaka University, 2-1 Yamadaoka, Suita, Osaka 565-0871, Japan*

(Received 8 December 2015; accepted 27 February 2016; published online 20 May 2016)

We evaluated the damage threshold of coating materials such as Mo, Ru, Rh, W, and Pt on Si substrates, and that of uncoated Si substrate, for mirror optics of X-ray free electron lasers (XFELs). Focused 1 μm (full width at half maximum) XFEL pulses with the energies of 5.5 and 10 keV, generated by the SPring-8 angstrom compact free electron laser (SACLA), were irradiated under the grazing incidence condition. The damage thresholds were evaluated by *in situ* measurements of X-ray reflectivity degradation during irradiation by multiple pulses. The measured damage fluences below the critical angles were sufficiently high compared with the unfocused SACLA beam fluence. Rh coating was adopted for two mirror systems of SACLA. One system was a beamline transport mirror system that was partially coated with Rh for optional utilization of a pink beam in the photon energy range of more than 20 keV. The other was an improved version of the 1 μm focusing mirror system, and no damage was observed after one year of operation. *Published by AIP Publishing.* [http://dx.doi.org/10.1063/1.4950723]

I. INTRODUCTION

The advent of X-ray free electron laser (XFEL) facilities[1,2] allows generation of extremely high intensity X-rays with ultra-short pulses, which are of considerable interest for several fields. However, high-intensity pulses can damage optical elements, potentially significantly degrading the beam quality. Thus, optical elements at XFEL facilities should exhibit sufficient damage tolerance and high-quality optical performance.

Total reflection mirrors are used in beamline transport mirror systems for conducting all of the fundamental spectrum and suppressing higher-order harmonics; they are also used in focusing mirror systems[3,4] for producing extremely high power-density X-ray pulses. To avoid damaging optical surfaces, the coating materials that are used for the total reflection mirrors at XFEL facilities are usually low-Z materials, such as carbon and B_4C. Although low-Z coating materials have a high tolerance owing to their low absorption and high reflectivity, a disadvantage of these materials is a small critical angle, yielding a small glancing angle and acceptance aperture. There has been an increasing demand for the use of metal coatings, which have large critical angles, to obtain high-throughput and high numerical aperture within a limited mirror length, working distance, and installation space. Recently, the damage thresholds of various optical materials have been reported for both normal and grazing incidence conditions in the extreme ultraviolet (EUV) and soft X-ray regions[5–13] and also in the hard X-ray region.[14–21]

In this paper, we systematically studied the damage thresholds of various coating materials. We used focused XFEL pulses from the SPring-8 angstrom compact free electron laser (SACLA),[2] with photon energies of 5.5 and 10 keV; these focused pulses were sufficient for inducing ablation. We studied metal (Mo, Ru, Rh, W, and Pt) coatings on Si substrates, as well as an uncoated Si substrate. We irradiated the samples by using multiple shots in the grazing incidence condition. Furthermore, we discuss the application of our results on metal-coated mirrors to a beamline plane mirror system and a focusing mirror system.

II. DAMAGE THRESHOLD FLUENCE FOR THE GRAZING INCIDENCE CONDITION

The irradiation tolerance of optical materials can be estimated by comparing the absorption dose with the melting dose. The melting dose has been considered as a reasonable guide for designing optical components.[22–24] Table I lists the calculated melting doses of some materials and also lists the damage threshold doses of some of these materials, measured under the normal incidence condition.[16] Previously, we have reported the damage threshold doses of Si, Rh, and Pt under the normal incidence condition. The melting doses of these materials were calculated from their thermodynamic properties, which accounted for their temperature-dependent heat capacity and the latent heat of melting.[25]

a)Author to whom correspondence should be addressed. Electronic mail: koyama@spring8.or.jp

TABLE I. The calculated melting doses of several materials and the measured threshold doses[16] under the normal incidence condition.

	Calculated melting dose (eV/atom)	Measured threshold dose (eV/atom)
Si	0.88	0.73 ± 0.04
Mo	1.20	...
Ru	1.16	...
Rh	0.90	0.79 ± 0.08
W	1.57	...
Pt	0.78	0.52 ± 0.09

For the grazing incidence condition, the damage threshold fluence can be calculated from the melting dose D_{th} as[22–24]

$$F_{\mathrm{th}} = \frac{D_{\mathrm{th}}\rho N_{\mathrm{A}} d}{A(1-R)\sin\theta}, \tag{1}$$

where ρ, N_A, A, R, and θ are the density, Avogadro's constant, the atomic weight, the reflectivity, and the glancing angle, respectively. The variable d is the energy deposition depth, given by $d = \sqrt{{d_x}^2 + {d_e}^2}$, where d_x is the X-ray penetration depth, calculated by using the angle-dependent absorption coefficient $\mu_g(\theta)$ as

$$\frac{1}{d_x} = \mu_g(\theta) = \frac{2\sqrt{2}\pi}{\lambda}\sqrt{\sqrt{(2\delta-\theta^2)^2+4\beta^2}+2\delta-\theta^2} \tag{2}$$

with the complex refractive index $n = 1 - \delta + i\beta$ and X-ray wavelength λ. The variable d_e is the electron collision length.[26]

Typically, in the hard X-ray region, the penetration depth below the critical angle is under 10 nm, owing to the formation of an evanescent field by total reflection. On the other hand, the electron collision length is in the 1–100 nm range,[26] and it depends on the material and on the kinetic energy of photoelectrons excited by kilo-electron volt X-rays. The energetic photoelectrons diffuse into a larger volume and deeper below the sample surface, so that the deposited energy is removed from the X-ray interaction region. Consequently, the energy deposition depth could become large. The effect of the energetic photoelectrons has been reported by using Monte Carlo simulations.[20]

III. EXPERIMENTAL SETUP

The experiments were performed at the SACLA beamline 3.[27] XFEL pulses (pulse duration, ~10 fs)[28] were generated by eighteen in-vacuum undulators that generated high-energy photons by a short undulator period. To conduct all of the fundamental spectrum and to suppress higher-order harmonics and gamma rays, a double plane mirror system (with carbon-coated surfaces) was used. We chose X-ray photon energies of 5.5 and 10 keV. Figure 1 shows the schematic of the experimental setup. The XFEL pulses were focused down to 1 μm full width at half maximum (FWHM) by using a focusing mirror system[3] consisting of elliptical mirrors (with carbon-coated surfaces), in Kirkpatrick-Baez geometry. A dedicated irradiation chamber,[16] equipped with high-precision translation stages and a rotation stage, was placed at the focal point

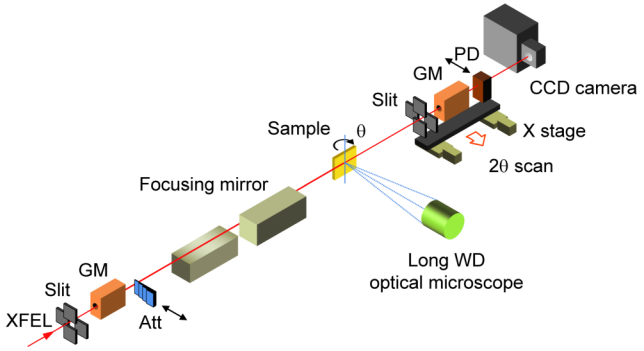

FIG. 1. Schematic drawing of the experimental setup. GM: gas monitor detector, Att: attenuator, PD: Si PIN photodiode detector.

of the focusing mirror system. The focused beam size was measured by using a knife edge scanning method. Incoming XFEL pulses were monitored by using a scattering-based intensity monitor (gas monitor) for normalizing shot-by-shot fluctuations.[29] The fluences were controlled by inserting Si and/or Al attenuators with various thicknesses, in front of the focusing mirrors.

Reflected pulses from the samples were measured by using two intensity detectors, consisting of a gas monitor and a Si PIN photodiode. A slit and the two detectors were arranged on an optical rail positioned by two motorized translation stages, to enable θ-2θ scanning by moving together with the sample rotation stage. A CCD detector was used for aligning the sample surface parallel to the focused beam axis. The sample surfaces were monitored by using a long working distance optical microscope from the surface normal direction. The samples were irradiated by multiple pulses at several glancing angles near the critical angle, and the number of shots was controlled by using a pulse selector.[30] The damage threshold fluences for the samples were evaluated by measuring the reflectivity degradation during the sample irradiation, as well as by inspecting the sample surface morphology by using a scanning probe microscope after the irradiation experiment.

IV. RESULTS

A. Threshold fluence at the 5.5 keV photon energy

We measured the threshold fluences of Mo, Ru, and Rh coated Si substrates, as well as that of an uncoated Si substrate, for the photon energy of 5.5 keV. A commercially available silicon (100) wafer was used as the substrate. The coating layers were deposited on the substrate by DC magnetron sputtering. For all samples, the coating layer was 50-nm-thick, and a 5-nm-thick chromium layer was inserted as an adhesive layer. During this experiment, SACLA generated pulses at 30 Hz. The series of focused XFEL pulses (100 and 1000 shots) were irradiated on the samples at several glancing angles. In addition, for Rh-coated Si, we also considered irradiation with 10^4 and 10^5 shots. The measured threshold fluences, reflectivities, and glancing angles are summarized in Table II, and the measured threshold fluences are plotted in Fig. 2 vs. the glancing angle. In Fig. 2, the solid and dashed lines denote

TABLE II. The measured glancing angles and the damage fluences at 5.5 keV.

	Critical angle (mrad)	Measured angle (mrad)	Measured reflectivity	Damage fluence (μJ/μm^2)
Si	5.7	2.0	0.96	1.2
		4.0	0.91	0.58
		5.7	0.74	0.095
		11.4	0.005	0.052
Mo	11.1	4.0	0.91	0.28
		8.0	0.76	0.088
		10.8	0.33	0.019
		20.9	0.003	0.024
Ru	12.2	4.0	0.90	0.28
		8.0	0.78	0.093
		12.2	0.33	0.012
		24.4	0.002	0.016
Rh	12.2	4.0	0.90	0.25
		8.0	0.76	0.051
		12.2	0.35	0.013
		24.4	0.002	0.014

the threshold fluence curves calculated from Eq. (1) with and without considering the electron collision length d_e. In this case, d_e was treated as a fitting parameter; thus, the obtained values of d_e for Si, Mo, Ru, and Rh were 35, 15, 15, and 10 nm, respectively. The fits were performed with a single value for d_e of each material for the entire angular range rather than fitting d_e at each point and averaging the result. As is clearly seen from Fig. 2, in the glancing angles below the critical angles, the electron collision length played a significant role in reducing the damage by one order of magnitude. Energetic photoelectrons that were excited in the samples' X-ray interaction regions transported the deposited energy into the material bulk. In addition, no damage was observed after a 5-h-long irradiation of the Rh-coated Si sample with an unfocused beam without any attenuators, under both the normal and grazing incidence conditions.

TABLE III. The measured glancing angles and the damage fluences at 10 keV.

	Critical angle (mrad)	Measured angle (mrad)	Measured reflectivity	Damage fluence (μJ/μm^2)
Si	3.1	2.1	0.97	11
		2.8	0.94	3.7
Mo	6.1	3.4	0.93	2.0
		4.6	0.80	0.85
Ru	6.7	3.7	0.87	1.9
		5.0	0.74	0.85
Rh	6.7	3.7	0.93	0.81
		5.5	0.84	0.35
		6.7	0.50	0.18
W	7.5	4.4	0.87	0.87
Pt	8.1	4.5	0.88	0.41
		6.1	0.81	0.24

B. Threshold fluence at the 10 keV photon energy

Similar to the irradiation with 5.5-keV-energy photons, threshold fluences of Mo, Ru, and Rh coated Si, as well as that of the uncoated Si, were measured for the irradiation with 10-keV-energy photons. In addition, we also irradiated W and Pt coated Si, because these materials have large critical angles, enabling to reflect high-energy X-rays at the same glancing angle. For all samples, the coating was 100-nm-thick, and a 5-nm-thick chromium layer was inserted as an adhesive layer. During this experiment, SACLA generated pulses at 10 Hz. The series of focused XFEL pulses (100 and 1000 shots) were irradiated on the samples at several glancing angles. In addition, for Rh, we performed irradiation with 10^4 shots. The measured threshold fluences, reflectivities, and glancing angles are summarized in Table III, and the measured threshold fluences are plotted in Fig. 3 vs. the glancing angle. Note that the lack of data points compared with the measurement of 5.5-keV-energy photons was due to limited measurement time. In Fig. 3, the solid and dashed lines denote the threshold

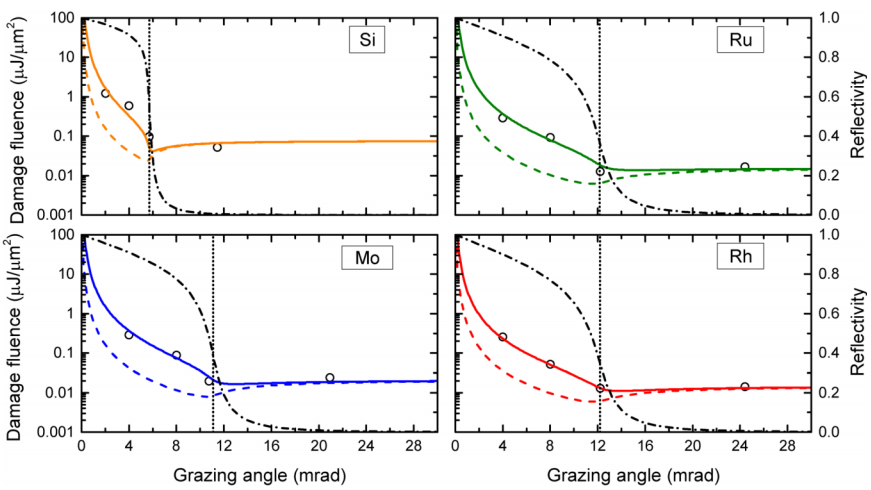

FIG. 2. Damage fluences of Si, Mo, Ru, and Rh at the irradiation with 5.5-keV-energy photons, plotted as a function of the grazing angle. Circles indicate the measured values. Solid and dashed lines show the thresholds with and without considering the electron collision length. Dashed-dotted lines indicate the reflectivity (right y axis). The critical angles are indicated with dotted vertical lines.

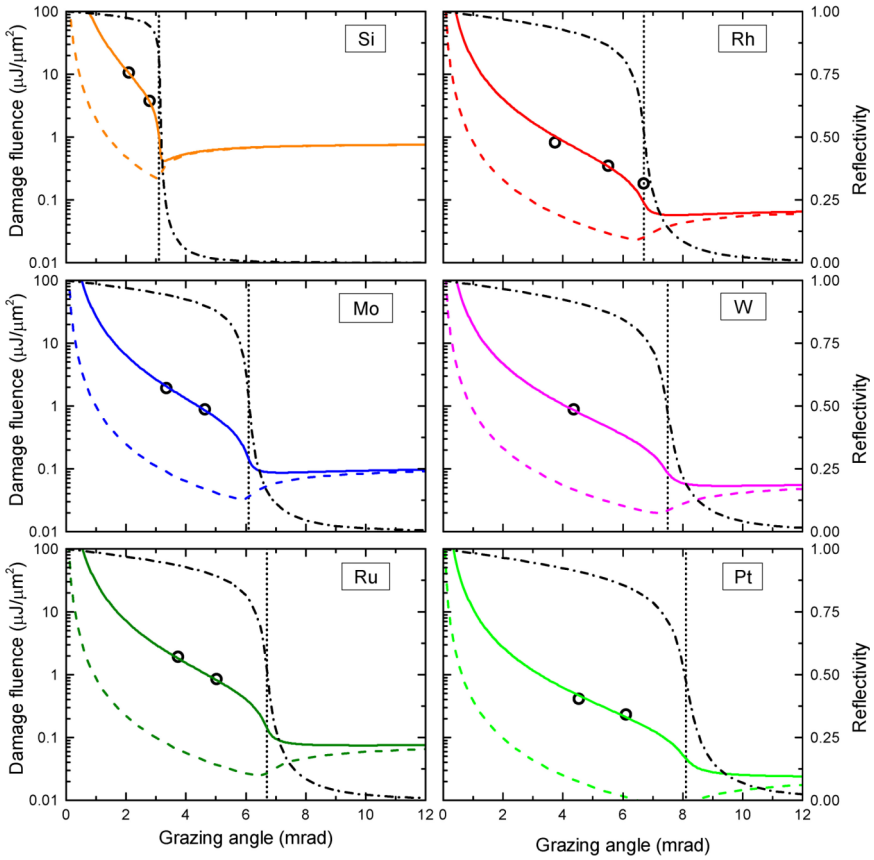

FIG. 3. Damage fluences of Si, Mo, Ru, Rh, W, and Pt at the irradiation with 10-keV-energy photons, plotted as a function of the grazing angle. Circles indicate the measured values. Solid and dashed lines show the thresholds with and without considering the electron collision length. Dashed-dotted lines indicate the reflectivity (right y axis). The critical angles are indicated with dotted vertical lines.

fluence curves calculated from Eq. (1) with and without considering the electron collision length d_e. Similar to the irradiation with 5.5-keV-energy photons, the parameter d_e was treated as a fitting parameter; the obtained d_e values for Si, Mo, Ru, Rh, W, and Pt were 100, 45, 50, 30, 30, and 35 nm, respectively. These electron collision length values were approximately threefold larger than those for the irradiation with 5.5-keV-energy photons. The energetic photoelectrons excited by more energetic X-rays are likely to have higher kinetic energy; thus, these energetic photoelectrons are likely to remove a larger amount of deposited energy from the X-ray interaction region and exhibit stronger diffusion. As a result, the difference between the damage threshold fluences with and without considering the electron collision length is larger than that for the irradiation with 5.5-keV-energy photons.

We also observed that for the glancing angles much larger than the corresponding critical angles (implying the normal incidence condition), the threshold fluences of Si, Rh, and Pt approached the values of 0.78, 0.072, and 0.023 $\mu J/\mu m^2$ that were previously measured for the normal incidence condition.[16]

V. APPLICATIONS OF METAL COATING MIRROR AT SACLA

For the SACLA mirror optics, we estimated the maximal fluence of an unfocused beam as ~0.0015 $\mu J/\mu m^2$ (beam diameter: ~600 μm FWHM, peak pulse energy: ~600 μJ) for the 5.5-keV-energy photons and ~0.006 $\mu J/\mu m^2$ (beam diameter: ~300 μm FWHM, peak pulse energy: ~600 μJ) for the 10-keV-energy photons. As is clearly seen from Figs. 2 and 3, the damage threshold fluences below the critical angles of the metal coatings were sufficiently higher than the unfocused beam fluences. We adopted Rh as a coating material for the mirror optics because it has no absorption edge in the 4–23 keV energy range and because it is a proven material used at the synchrotron radiation facility SPring-8. In what follows, we present the application of our results on this metal coating to two systems. One system is a double plane mirror system, and the other is a 1 μm focusing mirror system.

A. Double plane mirror system

We employed Rh coating in a beamline double plane mirror system placed at an optics hutch of beamline 3 of SACLA. Rh coating was partially coated on the mirror surface to enable optional utilization of a pink beam with photon energy range of more than 20 keV. The beamline optical system of SACLA basically consists of two sets of double plane mirrors and a double crystal monochromator in the optics hutch. Figure 4(a) shows the schematic of the double plane mirror system. Two mirror sets with different glancing angles totally reflect X-rays below the critical angle (cutoff energies). One set (M1 and M2a) has a 4 mrad glancing angle for lower-

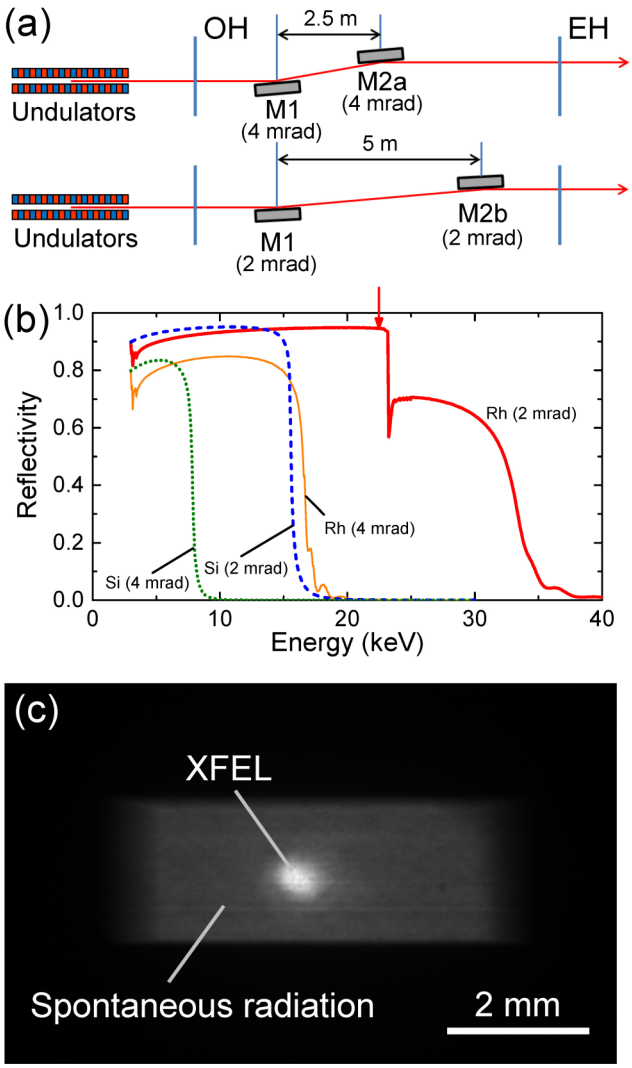

FIG. 4. (a) Schematic of the beamline plane mirror system. (b) The calculated reflectivity of the mirrors with Rh-coated Si and uncoated Si. The reflectivity curves were considered with double reflection. The red arrow indicates the photon energy of 22.5 keV. (c) The image of a typical 22.5-keV-energy beam, reflected by M1 and M2b with Rh-coated plane mirrors. The measured reflectivity at 22.5 keV was 92%, while the calculated reflectivity was 95%.

energy photons. The other one (M1 and M2b) has a small 2 mrad angle for higher-energy photons. The plane mirrors reduce the contribution of higher-order harmonics that have photon energy above cutoff energies.

Figure 4(b) shows the calculated reflectivity curves. The complex refractive index of the materials was obtained from atomic scattering factors given by Henke *et al.*[31] for the photon energy $E \leq 30$ keV and by Sasaki[32] for $E > 30$ keV. The reflectivity of Rh (50 nm)/Cr (5 nm)/Si substrate at 2 and 4 mrad, as well as that of uncoated Si substrate at 2 and 4 mrad, was calculated as a function of the X-ray energy. These curves were considered with double reflection. The cutoff energies were 7.5 and 15 keV at the Si surface set at the glancing angles of 4 and 2 mrad, as well as 16 and 33 keV at the Rh surface set at the glancing angles of 4 and 2 mrad, respectively.

The plane mirrors were installed in September of 2014. The measured (calculated) reflectivity was 77% (80%) at 15 keV using the 4 mrad system and 92% (95%) at 22.5 keV using the 2 mrad system. Figure 4(c) shows the image of a typical beam of 22.5-keV-energy photons. The XFEL beam can be observed at the center of the diverging spontaneous radiation from undulators limited by a rectangular front-end slit aperture. Although the measured intensity was as low as ~1 μJ, because the photon energy of 22.5 keV was close to the upper limit on the photon energy generated by SACLA, a pink beam with the energy region of above 20 keV can be utilized for users who require high-energy XFEL beams.

B. Improved 1 μm focusing mirror system

We also employed Rh coating in an improved version of the 1 μm focusing mirror system at SACLA. Improvement was needed to increase the throughput of XFEL pulses to a sample while maintaining its beam size at 1 μm, as well as maintaining its working distance and component (vacuum chamber, apparatus) size. Figure 5(a) shows the schematic of the improved version of the 1 μm focusing system that consists of two sets of mirrors. The mirror glancing angles can be set to either ~3.7 mrad or ~2.0 mrad by translating the mirrors to be operated. The former glancing angle can accept lower-energy XFEL photon pulses with a large divergence angle. Figure 5(b) shows a photograph of the mirrors arranged in the vacuum chamber. The mirror parameters are summarized in Table IV.

This focusing mirror system was installed in beamline 3 in October of 2014 and was also installed in beamline 2. The measured beam sizes at 10 keV were 0.85 (H) × 1.02 (V) μm^2 in the 2 mrad system and 0.84 (H) × 1.07 (V) μm^2 in the 4 mrad

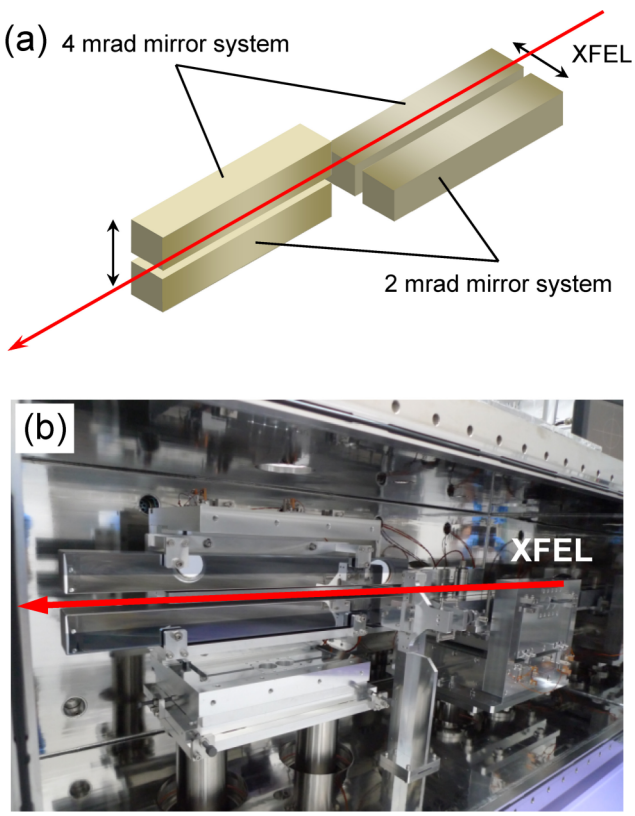

FIG. 5. (a) Schematic of an improved version of the 1 μm focusing system. (b) A photograph of the mirrors arranged in the vacuum chamber.

TABLE IV. New focusing mirror parameters.

	2 mrad system	4 mrad system
Surface profile	Elliptical cylinder	
Substrate material	Si	
Mirror substrate size	$600 \times 50 \times 50$ mm^3	
Surface coating	Rhodium 50 nm	
Graz. incidence angle	(H) 2.0 mrad (V) 2.1 mrad	(H) 3.7 mrad (V) 3.8 mrad
Spatial acceptance	(H) 1.20 mm (V) 1.26 mm	(H) 2.22 mm (V) 2.28 mm
Focal length	(H) 1.30 m (V) 1.95 m	

system. We observed that the focusing mirror throughput of the 10-keV-energy XFEL pulses to a sample improved from ~50% to >80% owing to the increased glancing angle and larger acceptance aperture yielded by the metal coating. It is important to note that no observable damage was incurred, because the focusing beam size of ~1 μm remained the same after one year of operation.

VI. SUMMARY

We evaluated the damage thresholds of coating materials such as Mo, Ru, Rh, W, and Pt on Si substrates, as well as of an uncoated Si substrate for XFEL mirror optics. The measured damage fluences below the critical angles were sufficiently high compared with the fluence of an unfocused beam at SACLA. Beamline transport mirror was partially coated with Rh for enabling optional use of the pink beam with photon energies above 20 keV. In addition, Rh coating was adopted for an improved version of the 1 μm focusing mirror system, and no damage was observed after one year of operation.

ACKNOWLEDGMENTS

The authors sincerely thank Hikaru Kishimoto and the SACLA engineering team for their help during the beam time. This work was performed at BL3 of SACLA with the approval of the Japan Synchrotron Radiation Research Institute (JASRI) (Proposal Nos. 2012B8052, 2013A8063, 2014A8051, and 2014B8074). This research was partially supported by a Grant-in-Aid for Scientific Research (S) (Grant No. 23226004) from the Ministry of Education, Sports, Culture, Science and Technology, Japan (MEXT).

[1]P. Emma, R. Akre, J. Arthur, R. Bionta, C. Bostedt, J. Bozek, A. Brachmann, P. Bucksbaum, R. Coffee, F.-J. Decker, Y. Ding, D. Dowell, S. Edstrom, A. Fisher, J. Frisch, S. Gilevich, J. Hastings, G. Hays, P. Hering, Z. Huang, R. Iverson, H. Loos, M. Messerschmidt, A. Miahnahri, S. Moeller, H.-D. Nuhn, G. Pile, D. Ratner, J. Rzepiela, D. Schultz, T. Smith, P. Stefan, H. Tompkins, J. Turner, J. Welch, W. White, J. Wu, G. Yocky, and J. Galayda, Nat. Photonics **4**, 641 (2010).

[2]T. Ishikawa, H. Aoyagi, T. Asaka, Y. Asano, N. Azumi, T. Bizen, H. Ego, K. Fukami, T. Fukui, Y. Furukawa, S. Goto, H. Hanaki, T. Hara, T. Hasegawa, T. Hatsui, A. Higashiya, T. Hirono, N. Hosoda, M. Ishii, T. Inagaki, Y. Inubushi, T. Itoga, Y. Joti, M. Kago, T. Kameshima, H. Kimura, Y. Kirihara, A. Kiyomichi, T. Kobayashi, C. Kondo, T. Kudo, H. Maesaka, X. M. Maréchal, T. Masuda, S. Matsubara, T. Matsumoto, T. Matsushita, S. Matsui, M. Nagasono, N. Nariyama, H. Ohashi, T. Ohata, T. Ohshima, S. Ono, Y. Otake, C. Saji, T. Sakurai, T. Sato, K. Sawada, T. Seike, K. Shirasawa, T. Sugimoto, S. Suzuki, S. Takahashi, H. Takebe, K. Takeshita, K. Tamasaku, H. Tanaka, R. Tanaka, T. Tanaka, T. Togashi, K. Togawa, A. Tokuhisa, H. Tomizawa, K. Tono, S. Wu, M. Yabashi, M. Yamaga, A. Yamashita, K. Yanagida, C. Zhang, T. Shintake, H. Kitamura, and N. Kumagai, Nat. Photonics **6**, 540 (2012).

[3]H. Yumoto, H. Mimura, T. Koyama, S. Matsuyama, K. Tono, T. Togashi, Y. Inubushi, T. Sato, T. Tanaka, T. Kimura, H. Yokoyama, J. Kim, Y. Sano, Y. Hachisu, M. Yabashi, H. Ohashi, H. Ohmori, T. Ishikawa, and K. Yamauchi, Nat. Photonics **7**, 43 (2013).

[4]H. Mimura, H. Yumoto, S. Matsuyama, T. Koyama, K. Tono, Y. Inubushi, T. Togashi, T. Sato, J. Kim, R. Fukui, Y. Sano, M. Yabashi, H. Ohashi, T. Ishikawa, and K. Yamauchi, Nat. Commun. **5**, 3539 (2014).

[5]N. Stojanovic, D. von der Linde, K. Sokolowski-Tinten, U. Zastrau, F. Perner, E. Förster, R. Sobierajski, R. Nietubyc, M. Jurek, D. Klinger, J. Pelka, J. Krzywinski, L. Juha, J. Cihelka, A. Velyhan, S. Koptyaev, V. Hajkova, J. Chalupsky, J. Kuba, T. Tschentscher, S. Toleikis, S. Düsterer, and H. Redlin, Appl. Phys. Lett. **89**, 241909 (2006).

[6]S. P. Hau-Riege, R. A. London, R. M. Bionta, M. A. McKernan, S. L. Baker, J. Krzywinski, R. Sobierajski, R. Nietubyc, J. B. Pelka, M. Jurek, L. Juha, J. Chalupský, J. Cihelka, V. Hájková, A. Velyhan, J. Krása, J. Kuba, K. Tiedtke, S. Toleikis, Th. Tschentscher, H. Wabnitz, M. Bergh, C. Caleman, K. Sokolowski-Tinten, N. Stojanovic, and U. Zastrau, Appl. Phys. Lett. **90**, 173128 (2007).

[7]S. P. Hau-Riege, H. N. Chapman, J. Krzywinski, R. Sobierajski, S. Bajt, R. A. London, M. Bergh, C. Caleman, R. Nietubyc, L. Juha, J. Kuba, E. Spiller, S. Baker, R. Bionta, K. S. Tinten, N. Stojanovic, B. Kjornrattanawanich, E. Gullikson, E. Plönjes, S. Toleikis, and T. Tschentscher, Phys. Rev. Lett. **98**, 145502 (2007).

[8]R. Sobierajski, D. Klinger, M. Jurek, J. B. Pelka, L. Juha, J. Chalupský, J. Cihelka, V. Hakova, L. Vysin, U. Jastrow, N. Stojanovic, S. Toleikis, H. Wabnitz, J. Krzywinski, S. Hau-Reige, and R. London, Proc. SPIE **7361**, 73610I (2009).

[9]A. R. Khorsand, R. Sobierajski, E. Louis, S. Bruijn, E. D. van Hattum, R. W. E. van de Kruijs, M. Jurek, D. Klinger, J. B. Pelka, L. Juha, T. Burian, J. Chalupsky, J. Cihelka, V. Hajkova, L. Vysin, U. Jastrow, N. Stojanovic, S. Toleikis, H. Wabnitz, K. Tiedtke, K. Sokolowski-Tinten, U. Shymanovich, J. Krzywinski, S. Hau-Riege, R. London, A. Gleeson, E. M. Gullikson, and F. Bijkerk, Opt. Express **18**, 700 (2010).

[10]S. P. Hau-Riege, R. A. London, A. Graf, S. L. Baker, R. Soufli, R. Sobierajski, T. Burian, J. Chalupsky, L. Juha, J. Gaudin, J. Krzywinski, S. Moeller, M. Messerschmidt, J. Bozek, and C. Bostedt, Opt. Express **18**, 23933 (2010).

[11]J. Gaudin, O. Peyrusse, J. Chalupský, M. Toufarová, L. Vyšín, V. Hájková, R. Sobierajski, T. Burian, S. Dastjani-Farahani, A. Graf, M. Amati, L. Gregoratti, S. P. Hau-Riege, G. Hoffmann, L. Juha, J. Krzywinski, R. A. London, S. Moeller, H. Sinn, S. Schorb, M. Störmer, T. Tschentscher, V. Vorlíček, H. Vu, J. Bozek, and C. Bostedt, Phys. Rev. B **86**, 024103 (2012).

[12]J. Gaudin, C. Ozkan, J. Chalupský, S. Bajt, T. Burian, L. Vyšín, N. Coppola, S. D. Farahani, H. N. Chapman, G. Galasso, V. Hájková, M. Harmand, L. Juha, M. Jurek, R. A. Loch, S. Möller, M. Nagasono, M. Störmer, H. Sinn, K. Saksl, R. Sobierajski, J. Schulz, P. Sovak, S. Toleikis, K. Tiedtke, T. Tschentscher, and J. Krzywinski, Opt. Lett. **37**, 3033 (2012).

[13]J. Krzywinski, D. Cocco, S. Moeller, and D. Ratner, Opt. Express **23**, 5397 (2015).

[14]C. David, S. Gorelick, S. Rutishauser, J. Krzywinski, J. Vila-Comamala, V. A. Guzenko, O. Bunk, E. Färm, M. Ritala, M. Cammarata, D. M. Fritz, R. Barrett, L. Samoylova, J. Grünert, and H. Sinn, Sci. Rep. **1**, 57 (2011).

[15]F. Uhlén, D. Nilsson, A. Holmberg, H. M. Hertz, C. G. Schroer, F. Seiboth, J. Patommel, V. Meier, R. Hoppe, A. Schropp, H. J. Lee, B. Nagler, E. Galtier, J. Krzywinski, H. Sinn, and U. Vogt, Opt. Express **21**, 8051 (2013).

[16]T. Koyama, H. Yumoto, Y. Senba, K. Tono, T. Sato, T. Togashi, Y. Inubushi, T. Katayama, J. Kim, S. Matsuyama, H. Mimura, M. Yabashi, K. Yamauchi, H. Ohashi, and T. Ishikawa, Opt. Express **21**, 15382 (2013).

[17]T. Koyama, H. Yumoto, K. Tono, T. Sato, T. Togashi, Y. Inubushi, T. Katayama, J. Kim, S. Matsuyama, H. Mimura, M. Yabashi, K. Yamauchi, and H. Ohashi, Proc. SPIE **8848**, 88480T (2013).
[18]J. Kim, T. Koyama, H. Yumoto, A. Nagahira, S. Matsuyama, Y. Sano, M. Yabashi, H. Ohashi, T. Ishikawa, and K. Yamauchi, Proc. SPIE **8848**, 88480S (2013).
[19]T. Koyama, H. Yumoto, K. Tono, T. Togashi, Y. Inubushi, T. Katayama, J. Kim, S. Matsuyama, M. Yabashi, K. Yamauchi, and H. Ohashi, Proc. SPIE **9511**, 951107 (2015).
[20]A. Aquila, R. Sobierajski, C. Ozkan, V. Hájková, T. Burian, J. Chalupský, L. Juha, M. Störmer, S. Bajt, M. T. Klepka, P. Dłużewski, K. Morawiec, H. Ohashi, T. Koyama, K. Tono, Y. Inubushi, M. Yabashi, H. Sinn, T. Tschentscher, A. P. Mancuso, and J. Gaudin, Appl. Phys. Lett. **106**, 241905 (2015).
[21]J. Kim, A. Nagahira, T. Koyama, S. Matsuyama, Y. Sano, M. Yabashi, H. Ohashi, T. Ishikawa, and K. Yamauchi, Opt. Express **23**, 29032 (2015).
[22]R. M. Bionta, LCLS Technical Note No. LCLS-TN-00-3, 2000.
[23]R. A. London, R. M. Bionta, R. O. Tatchyn, and S. Roesler, Proc. SPIE **4500**, 51 (2001).
[24]M. Yabashi, A. Higashiya, K. Tamasaku, H. Kimura, T. Kudo, H. Ohashi, S. Takahashi, S. Goto, and T. Ishikawa, Proc. SPIE **6586**, 658605 (2007).
[25]See http://webbook.nist.gov/chemistry/ for NIST Chemistry WebBook; NIST Standard Reference Database Number 69.
[26]E. J. Kobetich and R. Katz, Phys. Rev. **170**, 391 (1968).
[27]K. Tono, T. Togashi, Y. Inubushi, T. Sato, T. Katayama, K. Ogawa, H. Ohashi, H. Kimura, S. Takahashi, K. Takeshita, H. Tomizawa, S. Goto, T. Ishikawa, and M. Yabashi, New J. Phys. **15**, 083035 (2013).
[28]Y. Inubushi, K. Tono, T. Togashi, T. Sato, T. Hatsui, T. Kameshima, K. Togawa, T. Hara, T. Tanaka, H. Tanaka, T. Ishikawa, and M. Yabashi, Phys. Rev. Lett. **109**, 144801 (2012).
[29]K. Tono, T. Kudo, M. Yabashi, T. Tachibana, Y. Feng, D. Fritz, J. Hastings, and T. Ishikawa, Rev. Sci. Instrum. **82**, 023108 (2011).
[30]T. Kudo, T. Hirono, M. Nagasono, and M. Yabashi, Rev. Sci. Instrum. **80**, 093301 (2009).
[31]B. L. Henke, E. M. Gullikson, and J. C. Davis, At. Data Nucl. Data Tables **54**, 181 (1993).
[32]S. Sasaki, KEK Report 88-14, 1989.